

A SIMPLE MODEL OF THE AIR PERMEABILITY OF PAPER

Paul Shallhorn and Norayr Gurnagul

FPIInnovations – Paprican Division, 570 St. John's Blvd., Pointe-Claire, QC,
Canada H9R 3J9

ABSTRACT

We have developed a simple model of the air permeability of paper and shown that it is in reasonable agreement with experimental results for softwood chemical pulps. The permeability is given as a function of fibre external height and width and fibre volume fraction including the lumen volume if present. The most important conclusion from the model is that the average fibre thickness in the paper is the critical fibre property controlling air permeability. In fact, the theory predicts that the sheet permeability is roughly proportional to the fourth power of the fibre thickness.

INTRODUCTION

Air permeability is an important property in the conversion of sack paper, i.e., high air permeability facilitates the removal of entrained air during filling of the sack. It is one of the two key properties of sack paper, the other being tensile energy absorption. A desirable goal from the fundamental point of view is to predict the permeability of paper from basic fibre properties using a simple model.

The modeling of air permeability of paper has historically been an application of the Kozeny-Carman equation which models the paper structure as a bundle of parallel identical cylindrical capillaries oriented in the direction of the air flow. The apparent flow through the sheet is given as a function of the

void volume fraction, the radius of the capillaries, and a tortuosity factor to account for the fact that the real flow channels are non-uniform and not parallel. The limitation here is that the fibre parameters leading to the given permeability cannot be deduced from the assumed pore radius and that the tortuosity factor for anisotropic porous media such as paper cannot be deduced from first principles and becomes in many cases a factor to fit theoretical data to experimental data.

In recent times, permeability modeling consists of a fibre network, constructed by numerical algorithms, and a calculation of the flow through the network by lattice-Boltzmann hydrodynamics [1, 2]. The limitation is that the accuracy of the calculations depends on the size of the simulation box of fibres which puts serious demands on the computing power available. Also, the results of the calculations must be interpreted carefully to extract a clearer understanding of the permeability of paper.

Another recent approach is to construct a two-dimensional matrix of infinitely long solid rods of different cross-section (circular, elliptical, or rectangular) and calculate the creeping flow through these structures [3–5]. In this case, the Navier-Stokes equations for creeping flow are solved either analytically or numerically so that no resolution problems are incurred. Rectangular fibres appear to be the best approximation to flattened wood fibres [6]. Nilsson and Stenstrom [5] in 1997 calculated using the numerical approach the permeabilities through a regular array of parallel non-contacting rectangular fibres of width-to-thickness ratio of 3.5 and found the results to be in good agreement with measured permeabilities through handsheets of unbeaten softwood kraft over a range of porosity levels (void volume fraction 0.5–0.9). In 2001, Nilsson [7] presented a simple model of fluid permeability using Poiseuille's equation for the rectangular channels through the array of rectangular fibres considered in [5] and found the results to be in excellent agreement with the rigorous solution of Navier-Stokes equations for creeping flow [5].

In this report, the Nilsson model is utilized but with a somewhat more realistic model of paper as planar arrays of parallel rectangular fibres contacting each other with alternative arrays oriented at right angles to each other. This more physical approach assumes firstly an explicit fibre structure which leads to an explicit pore structure through which air permeates. This model of paper structure is the same as that adopted by Page and Seth in their work on elastic modulus of paper [8]. Although reference [1] has shown that permeability is affected significantly with z-directional fibre orientation, the model used here assumes no z-directional fibre orientation since the literature indicates for sheets made at low consistency little such orientation of the fibres as a whole although small segments may orient into the z-direction. In

addition the model utilizes a regular array of fibres and therefore does not consider the effects on permeability of pulp fines, paper formation, and fibre orientation. This paper explores the permeability calculated from this model in relation to experimental values for sheet and fibre properties of various softwood chemical pulps.

MODEL

Theory

The fluid flow through a porous structure is assumed generally to follow Darcy's equation:

$$V = Q / A = -\frac{K}{\mu} \frac{dp}{dz} \quad (1)$$

V is the fluid flow velocity (m/s) in the z -direction, Q is the volumetric flow (m^3/s), A is the cross-sectional area of flow (m^2), μ is the viscosity of the fluid ($\text{N}\cdot\text{s}/\text{m}^2$), dp/dz is the gradient of pressure in the z -direction (Pa/m^2), and K is termed the permeability coefficient or constant (m^2) of the structure. The air permeability constant, K , of a sheet of paper may be calculated knowing the Gurley or Parker air volumetric flow (e.g., mL/s), the viscosity of air, the caliper of the sheet, and the pressure drop and sheet area used by the Gurley or Parker instrument.

Figure 1a shows the model paper structure for which the goal is to calculate the permeability constant K from the air flow in the transverse and in-plane directions. In Figure 1b of the model of paper structure, B is the distance between fibre centres (m), and b and h are the external fibre width (m) and thickness (m), respectively. Note that z -directional flow through the sheet is just a multiple of the flow through the elementary or repeating cross-sectional area B^2 . In the model, the fibre length is considered very much greater than B , b , and h and its effect is ignored. In Figures 1a and 1b, the fibres are truncated for clarity of presentation. It is recognized that b and h are functions of the fibre morphology and the consolidation of the paper structure. For an actual fibre, a lumen void may exist within the external dimensions. It is easily shown for one layer of fibres that the fibre volume fraction, ϕ is given by $(bhL)/(BhL)$ where L is the fibre length, or simply b/B . Since all layers of fibres are identical, ϕ for the whole structure is also b/B .

The apparent z -directional fluid flow through the structure in Figure 1b is considered to be made up of two microscopic flows: a transverse flow in the square channel, defined in cross-section by the free fibre length ($B-b$) for the

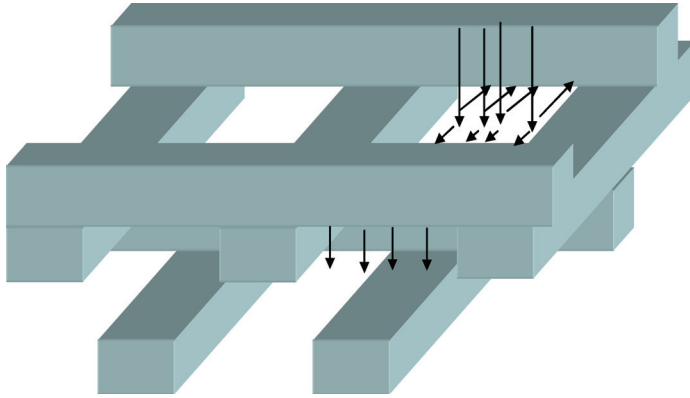


Figure 1a. Model geometry (three-dimensional view).

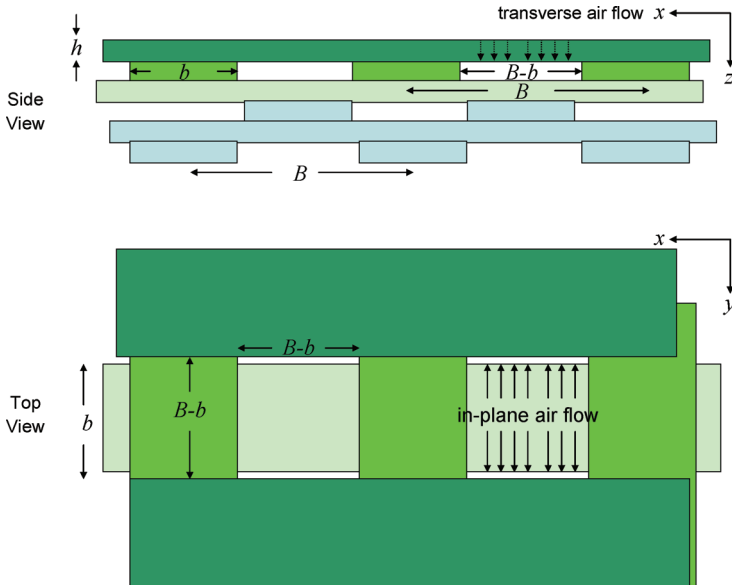


Figure 1b. Model geometry.

square side, and in length by h ; and an in-plane flow in two opposite rectangular channels, defined in cross-section by length $(B-b)$ and width h , and in depth by $b/2$. The apparent flow v is considered to be through the square area defined by side B .

Hagen-Poiseuille flow of an incompressible viscous fluid is assumed for air permeation within the pore structure of the paper. The compressibility of air can be ignored since the total pressure drop in the air permeability testers, such as the Gurley densometer, used for air permeability testing of paper are well within the limit of 2 kPa for a volume change of 1 % [9]. The pressure drop within the paper pores is much less than the total drop across the paper thickness. The volumetric flow rate Q of an incompressible viscous fluid of mean velocity v in a rectangular channel of cross-section defined by long dimension c and short dimension d is given by the equation [10];

$$Q = -\frac{cd^3}{12\mu} \frac{dp}{dz} \cdot F\left(\frac{c}{d}\right) \quad (2)$$

where dp/dz is the pressure gradient in the z -direction, the direction of flow. $F(c/d)$ is a function of the c/d ratio [10]:

$$F\left(\frac{c}{d}\right) = 1 - \frac{192d}{\pi^5 c} \cdot \sum_{i=1,3,5}^{\infty} \left(\frac{\tanh\left(\frac{i\pi c}{2d}\right)}{i^5} \right) \quad (3)$$

For $c \gg d$, F approaches unity, and for $c/d = 1$, i.e. a square channel, $F = 0.42$ approximately.

Thus, using equation 2, the transverse volumetric flow by the pressure gradient $\Delta P_1/h$ is given by

$$vB^2 = -\frac{F_1(B-b)^4}{12\mu} \left(\frac{\Delta P_1}{h} \right) \quad (4)$$

where the left side of the equation is the apparent macroscopic flow through the elementary area B^2 and the right side is the actual microscopic flow through the pore area $(B-b)^2$. The value of F , i.e. equation 3, for this flow, F_1 , is equal to 0.42 since the pore area is square with side $(B-b)$.

In the next layer below, the transverse microscopic flow above is split into two in-plane microscopic flows by a pressure gradient $\Delta P_2/(b/2)$ through two rectangular channels. This statement is equivalent to the following equation

$$\frac{vB^2}{2} = -\frac{F_2(B-b)h^3}{12\mu} \left(\frac{\Delta P_2}{(b/2)} \right) \quad (5)$$

where $F_2 = F((B-b)/h)$. For the range of sheet apparent density and range of b and h considered in the case studies given later, $(B-b)/h$ is roughly 7, and F_2

is therefore approximately 0.9. As a matter of fact, F_2 varies little with $(B-b)/h$, having the values 1 to 0.8 for values of $(B-b)/h$ from infinity to 3.

Finally, the macroscopic flow through the two elementary layers is considered an application of Darcy's equation as follows

$$vB^2 = - \frac{KB^2}{\mu} \frac{(\Delta P_1 + \Delta P_2)}{2h} \quad (6)$$

Combining equations 4, 5, and 6, one obtains

$$\frac{1}{K} = \frac{6\phi^2}{(0.42) b^2 (\phi^{-1} - 1)^4} + \frac{3b^2}{2 (0.9) \phi(1 - \phi) h^4} \quad (7)$$

where $\phi = b/B$ in the model. The first term in the right side of equation 7 is due to the transverse flow and the second term is due to the in-plane flow. Note that the numerical values of F_1 and F_2 have been inserted in this equation.

The calculation of the experimental value of the fibre fraction, ϕ , from simply the ratio of sheet density and cell wall density tends to underestimate ϕ since the lumen volume if present is not accessible to air flow and lowers sheet density. The ratio of the lumen cross-sectional area, LA , to the cell wall area, A , can vary from zero to 0.6 times for well beaten to unbeaten softwood kraft according to unpublished results of Jang [10]. In general, ϕ can be expressed as $(1 + LA/A)\rho/\rho_f$ where ρ = sheet density and ρ_f is cell wall density (here 1.55 g/cm^3). It will be shown that the second term of equation 7 is the dominant term and it can be shown that this term is relatively insensitive to the value of ϕ around the usual value of $\phi \sim 0.5$.

For flattened fibres in a planar sheet of randomly oriented fibres, Perkins [12] derives the centroidal distance (m) between fibres, B , as;

$$B = \frac{\pi b \rho_f}{4\rho} \cong \frac{0.8b\rho_f}{\rho} \quad (8)$$

where b is the fibre width (m), ρ is the sheet density (kg/m^3) and ρ_f is cell wall density (kg/m^3). The above analysis of the model for orthogonally oriented fibres gives $B = b \rho_f/\rho$ for flattened fibres with no lumen volume. The close agreement of values of the centroidal distance, $B \approx 0.8 b \rho_f/\rho$ for random sheets, and $b \rho_f/\rho$ for the model here, indicates that the assumption of a network of orthogonally oriented fibres gives relations similar to a network of randomly oriented fibres.

At this point, it is instructive to insert typical values of fibre parameters in equation 7 to see the relative value of the two terms in this equation, and to see if a reasonable value of the permeability constant, K , results. For unbeaten black spruce [13], values of h were measured as $6.5 \mu\text{m}$ at standard wet pressing pressure. Assuming a fibre perimeter of $80 \mu\text{m}$, b becomes $33.5 \mu\text{m}$. The sheet density was 0.58 g/cm^3 . For unbeaten pulp, LA/A is approximately 0.6 so that ϕ equals 0.60. Therefore $1/K$ can be calculated from equation 7 as:

$$\frac{1}{K} = (0.2 + 4.4) \times 10^{12} \text{ m}^{-2} \quad (9)$$

The first term representing the resistance of the model fibre structure to the transverse microscopic flow is quite small compared to the second term which represents the resistance of the structure to the in-plane microscopic flow. This is because the ratio of the second flow to the first flow is roughly proportional to $(h/b)^4$ which is much less than unity since $h \ll b$. Since the microscopic transverse and in-plane flows are in series, the in-plane flow, being by far the smallest, is the limiting flow. This means that the permeability of the paper is largely determined by the fibre thickness which controls the microscopic in-plane flow component of the apparent flow. The importance of fibre thickness in determining fibre sheet properties has been pointed out by Sampson and Urquhart [14] for pore size distribution and by Termonia [15] for permeability. This also explains why the analysis of the transverse flow component only by Corte and Lloyd was not very fruitful in modeling the air permeability of paper [16]. From equation 9, $K = 2.2 \times 10^{-13} \text{ m}^2$ which agrees roughly with values quoted in the literature [2, 5].

In the above calculation, $80 \mu\text{m}$ was assumed as the perimeter of a fibre. The value of $80 \mu\text{m}$ follows from the work of Seth [17] on low yield softwood kraft pulps who found using image analysis techniques that the fibre wall thickness was proportional to the fibre coarseness. The proportionality factor gives a constant fibre perimeter of about $80 \mu\text{m}$ ($\pm 10\%$) for the eight different softwood species considered by Seth. More recent work by Seth [6] using confocal laser scanning microscopy (CLSM) gives mean fibre outer perimeters of 68 to $86 \mu\text{m}$ for six softwood kraft pulp species. For simplicity, the assumption of a softwood kraft perimeter of $80 \mu\text{m}$ will be used for all softwood chemical fibres discussed in this report. It is also noted that with flattened fibres $b \gg h$ so that fractional change in b with wet pressing or refining is very much less than the fractional change in h .

Some limitations of the model may be specified here. It assumes no deflection by wet pressing of the fibres from their initial plane into adjacent layers

of fibres which would restrict flow further. It also assumes no corrections for abrupt changes in flow directions from transverse to in-plane and back to transverse. Finally, it does not account for the significant influence of fines on air permeability.

MODEL VALIDATION

To validate the model, one needs to compare the experimental permeability of a paper to the theoretical permeability predicted using equation 7 and values of b , h , and ϕ for that paper. There are little data in the literature on the air permeability of paper as well as the cross-sectional dimensions of fibres and the fibre fraction of that paper. However, four case studies follow, using both published and unpublished data.

Case 1

The only published work which contains values of fibre thickness of chemical pulp at various wet pressing pressures and sheet density is that of Görres *et al.* [13] for the long fibre fraction (14/28 Bauer-McNett) of eastern Canadian softwood kraft pulp. Fibre thickness was measured using a stylus profilometer. The relation between Gurley flow Q (mL/s), sheet grammage G (g/m²) and sheet density ρ (g/cm³) and the permeability K (m²) is assumed to follow the modified form of Darcy's law, equation 1, as follows:

$$Q = vA = \frac{-KA}{\mu} \left(\frac{dp}{dz} \right) = \frac{-KA}{\mu} \left(\frac{\text{pressure drop}}{\text{sheet thickness}} \right) \quad (10)$$

where A is the measurement (apparent) area of the Gurley instrument (6.45×10^{-4} m²), the pressure drop is 1.22×10^3 Pa/m², sheet thickness = sheet grammage/density, and μ is 1.8×10^{-5} N·s/m² for air at room temperature. Putting this together, we obtain

$$Q = 4.3 \times 10^{16} K \left(\frac{\rho}{G} \right) \quad (11)$$

The data from reference 13 are summarized in Table I.

A model Gurley flow was calculated for each pressure with equations 7 and 11 using the data in Table I. Figure 2 shows that the calculated Gurley flow follows the same trend with sheet density as the experimental value. The calculated values are generally higher but the experimental values are well

Table I. Fibre and sheet properties from Gorres *et al.* [13] of the long fibre fraction of eastern Canadian softwood kraft. The mean fibre thickness values have a standard deviation of about 2 μm .

<i>Pressure kPa</i>	<i>Mean fibre thickness μm</i>	<i>Grammage g/m^2</i>	<i>Sheet density g/cm^3</i>	<i>Gurley flow* mL/s</i>
350	6.5	60.3	0.58	42
860	5.5	60.6	0.67	20
2240	4.2	60.5	0.70	13
4830	3.9	60.7	0.75	7

* Unpublished data from R. Amiri, Paprican.

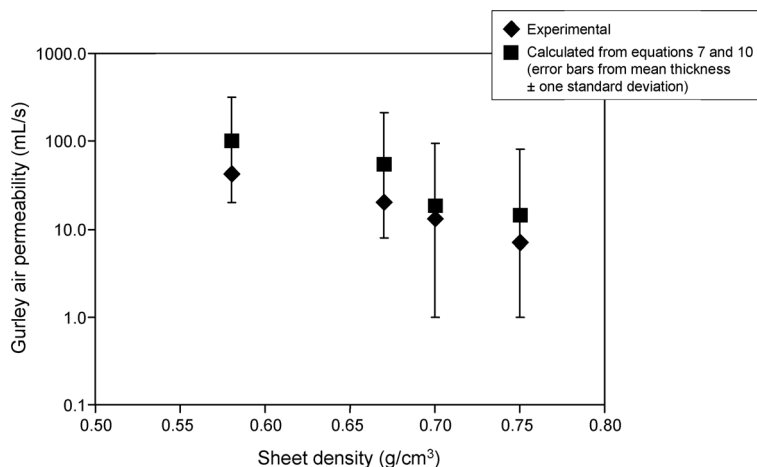


Figure 2. Comparison of calculated Gurley air permeability with experimental values of Eastern Canadian softwood kraft [13].

within the error bars calculated from assuming the fibre thickness to be $\pm 2 \mu\text{m}$ [13] of the mean value in Table I. The lack of closer agreement of the calculated and experimental values is a result of the limitations and assumptions in such a simple model and error in the values of fibre thickness and sheet properties. Among other limitations, the model does not include deflection of fibres in the thickness direction which would result in smaller but more in-plane channels and hence smaller flow values possibly. Equation 7 is very sensitive to the value of h (fibre thickness). The fibre thickness value in Table 1 if smaller would give better agreement in Figure 2. This agrees with

the conclusion of Görres *et al.* [13] that their fibre thickness values were on the high side.

Case 2

Never dried unbleached kraft pulps of different species and coarseness values were refined in a PFI mill to various freeness values and the resulting pulp and handsheet properties measured [17]. As the pulp is refined, the fibres will collapse more under standard wet pressing conditions. Jang using CLSM has shown that the ratio of lumen area to fibre wall area (LA/A) for black spruce kraft pulp beaten for 0, 1000, and 4000 PFI revolutions was 0.6, 0.4, and 0.2, respectively [11]. No freeness values were available. To obtain freeness values corresponding to these PFI revolutions, unpublished data from the work of reference [17] on a black spruce pulp of similar yield were used. These PFI revolutions of 0, 1000, and 4000 correspond to about 700, 660 and 570 CSF, respectively. The assumption is made that these freeness values are valid for this analysis. Jang also found that a western Canadian softwood kraft beaten to 250 CSF had a value of LA/A of 0.01 [18]. The assumption will be made that the LA/A at the given freeness values above is the same for all softwood kraft pulps considered here. This assumption is supported by the conclusion of Jang and Seth [6] that wood pulp fibres of different species prepared similarly by the kraft chemical process have similar collapse behaviours.

For a rectangular fibre of a given double wall thickness, t_{2w} , and outer dimensions b and h , $LA = (b-t_{2w})(h-t_{2w})$ and $A = bh-LA$. Thus,

$$\frac{LA}{A} = \left[\frac{bh}{(b-t_{2w})(h-t_{2w})} - 1 \right]^{-1} \quad (12)$$

Using values of LA/A of 0.6, 0.4, 0.2 and 0.0 above, values of t_{2w} from [17], and assuming the fibre perimeter, $2b + 2h$, equals $80 \mu\text{m}$ for all softwood fibres, values of h may be calculated from equation 12 for LA/A .

Table II below gives the values of coarseness, C , t_{2w} , and interpolated values of Gurley flow for 600 and 450 CSF along with the values of the model rectangular fibre thickness, h , calculated from equation 12 above. The values of Gurley flow, model fibre thickness, h , and sheet density at 600 and 450 CSF are interpolated from plots of flow, h and sheet density versus freeness over 700 to 250 CSF. The experimental values of freeness, sheet density and Gurley flow used are from unpublished data of reference [17].

In Figure 3, the experimental values of Gurley flow at 600 and 450 CSF for the various pulps are compared to values calculated from equations 7 and 11

Table II. Properties of softwood kraft pulps.

		<i>Western red cedar</i>	<i>Black spruce</i>	<i>Douglas fir</i>	<i>Jack pine</i>	<i>Sitka spruce</i>	<i>Loblolly pine</i>
C, $\mu\text{g/m}$		100	123	189	137	155	195
t_{2w} , μm		1.65	2.26	3.39	2.48	2.86	3.49
Gurley flow	600 CSF	1.3	6	22	8.8	10	28
mL/s							
Gurley flow	450 CSF	0.5	2	13	3	2	5.2
mL/s							

<i>CSF</i>	<i>LA/A</i>	<i>h, μm</i>	<i>h, μm</i>	<i>h, μm</i>	<i>h, μm</i>	<i>h, μm</i>	<i>h, μm</i>
700	0.6	2.7	3.8	5.8	4.2	4.8	6.0
660	0.4	2.5	3.2	5.0	3.6	4.1	5.0
570	0.2	2.0	2.7	4.2	3.0	3.5	4.3
250	0.0	1.7	2.3	3.4	2.5	2.9	3.5
600		2.2	2.8	4.4	3.2	3.7	4.5
450		1.8	2.3	3.5	2.7	3.0	3.6

<i>CSF</i>	<i>Sheet density, g/cm^3</i>						
600	0.69	0.69	0.61	0.69	0.68	0.63	0.63
450	0.74	0.73	0.63	0.71	0.71	0.64	0.64

using the data in Table II. A grammage of 60 g/m^2 was assumed in this calculation since standard handsheet data were used. The calculated values of Gurley flow at 600 CSF lie about 20% below the measured values indicating that the calculated values of h are slightly too small. The agreement of the calculated and measured values at 450 CSF is somewhat fortuitous. The effect of fines and fibre deflection in the z-direction may reduce the measured Gurley flow to match the calculated value which is based on fibres only. Nevertheless, the agreement of calculated and measured values of flow as well as their trend with coarseness is reasonable considering the assumptions made. It is also apparent from the graph and table that increasing coarseness increases Gurley flow particularly at the higher freeness. Based on the model, this is due in part to the greater change in fibre thickness with increasing coarseness at 600 CSF versus 450 CSF. At the lower freeness, the fibre has collapsed to the point that the lumen area is quite small and does not affect fibre thickness.

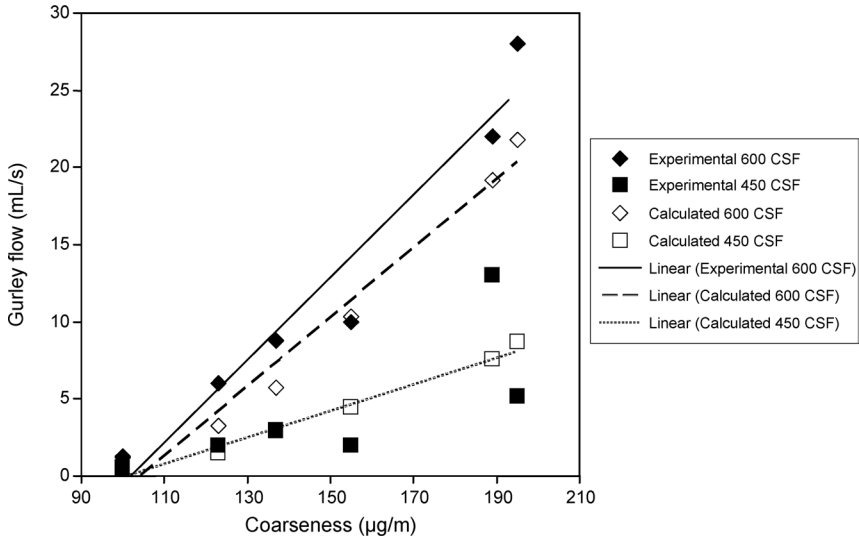


Figure 3. Comparison of calculated Gurley air permeability for pulps of different coarseness and freeness.

Case 3

A study on high-consistency refining (HCR) of kraft pulp for sack paper also included atmospheric and pressurized refining of the same pulp [19]. Pressurized HCR gives higher sheet air permeability at the same tensile energy absorption (TEA) than atmospheric HCR. Table III compares the effect of

Table III. Comparison of the effect of atmospheric and pressurized high consistency refining (HCR) on air permeability and measured and calculated fibre heights.

	<i>Atmospheric HCR 1800 RPM 336 kW·h/t</i>	<i>Pressurized HCR 1800 RPM 391 kW·h/t</i>
Gurley Permeability, mL/s	5.8	32
Grammage, g/m ²	93.4	84.3
Apparent density, g/cm ³	0.597	0.558
Fibre height by Image	5.6	6.4
Analysis, µm		
Standard Deviation, µm	1.0	1.4
Fibre height calculated with model, µm	3.7	5.5

atmospheric and pressurized HCR on Gurley air permeability and the theoretical fibre thickness calculated with the model equations to give the measured Gurley value. A measured value of fibre thickness by image analysis of the handsheets is also included. The image analysis was done on the scanning electron micrographs of handsheet cross-sections using Image Pro-Plus software (version 4.0) from Media Cybernetics.

The agreement between measured and calculated values is satisfactory considering the large standard deviation of the measured values. Also, the image analysis signal was filtered to reduce noise so that fibre thicknesses less than about two microns were not measured; therefore, the actual average measured fibre thicknesses would be less than the values in Table III and closer in value to the calculated thicknesses using the model.

It is seen that for the same specific energy pressurized HCR gives a higher Gurley volumetric flow rate and higher theoretical fibre thickness than the corresponding values for atmospheric HCR. It is conjectured that the lower water retention value achieved in pressurized HCR results in a less collapsed fibres in the bonded state after pressing and drying [19].

Case 4

In a laboratory experiment, unbeaten Douglas Fir kraft pulp was added to black spruce kraft pulp beaten to 430 mL CSF in a PFI mill. It is noted that Douglas fir is much coarser and therefore a less collapsible fibre than black spruce and was expected to make the resulting handsheets more porous. The mixture of 90% black spruce and 10% Douglas fir resulted in a handsheet increase of Gurley permeability of 70%, from 0.47 (Black Spruce alone) to 0.80 mL/s of the mixture. This large increase results from the fact that permeability is predicted by the model to be roughly proportional to the fourth power of the fibre thickness. This is seen from equation 7 for the permeability factor, K , where the second term, involving the fourth power of the fibre thickness (assuming the change in fibre width is not significant), has shown to be dominant. To determine the effect of the admixture of Douglas fir to the black spruce on permeability, the mean of the fourth power of the fibre thickness of the pulp mixture is calculated. This mean of the mixture will be then compared as a ratio to the fourth power of the fibre thickness of the black spruce itself. This ratio is predicted by the model to be similar to the ratio of the Gurley permeabilities of the mixture to black spruce alone.

The mean of any fibre property, here $\langle h^4 \rangle$, the mean of the fourth power of the mixture fibre thickness, in such a mixture of two pulps, is calculated from the theoretical discussion in [20]:

$$\langle h^4 \rangle = \frac{(\lambda_1 h_1^2 + \lambda_2 h_2^2)^2}{(\lambda_1 + \lambda_2)^2} \quad (13)$$

where $\langle h^4 \rangle$ is the mean of the fourth power of the mixture fibre thickness, and λ_i and h_i are the total fibre length and fibre thickness respectively of pulp is $i = 1, 2$ in the mixture pulp. This expression assumes that fibre collapse which dictates fibre thickness occurs mainly by wet pressing at fibre crossings whose number is proportional to the square of the total fibre length of a given pulp type. Since λ_i is proportional to w_i/C_i , where w_i and C_i are the weight fractions and fibre coarseness respectively of the two component pulps in the mixture, equation 13 becomes:

$$\langle h^4 \rangle = \frac{\left(\frac{w_1 h_1^2}{C_1} + \frac{w_2 h_2^2}{C_2} \right)^2}{\left(\frac{w_1}{C_1} + \frac{w_2}{C_2} \right)^2} \quad (14)$$

Substituting $h_1 = 2.3 \mu\text{m}$ (black spruce beaten to 450 CSF), $C_1 = 123 \mu\text{g/m}$, $h_2 = 5.8 \mu\text{m}$ (unbeaten Douglas fir), $C_2 = 189 \mu\text{g/m}$ from Table II, and $w_1 = 0.9$ and $w_2 = 0.1$, $\langle h^4 \rangle = 51.9 \mu\text{m}^4$. Therefore, the theoretical ratio of the permeability of the mixture to that of black spruce alone will be approximately $51.9/(2.3)^4$ or 1.9 to be compared to the experimental ratio of (0.80/0.47) or 1.7. This agreement is satisfactory considering the assumptions made. This indicates that small admixtures of coarser pulp can give significant increases in air permeability because of the fourth power sensitivity of permeability to fibre thickness. This result has wider implications. In this work, the effect of the fibre thickness distribution has not been considered. This distribution, although unknown, has non-negative and finite values of the ordinate (fibre thickness value extending from the totally collapsed fibre thickness to the totally uncollapsed fibre thickness), and is likely not skewed to smaller ordinate values. In this case, $\langle h^4 \rangle$ is equal to or greater than $\langle h \rangle^4$, the mean raised to the fourth power. Thus, the theoretical values of permeability calculated from the mean alone are likely underestimating the permeability if the fibre height distribution were to be taken into account.

CONCLUSION

A simple model of the air permeability of paper has been developed and shown to be in reasonable agreement with experimental results for softwood chemical pulps considering the simplicity of the model and experimental

error in the data used for validation. The permeability is given as a function of fibre external height and width and fibre volume fraction including the lumen volume if present. The model has no need of an assumption of a tortuosity factor used in models based on the Kozeny-Carman relation. The most important conclusion from the model is that the average fibre thickness in the paper is the critical fibre property controlling air permeability. In fact, the theory predicts that the sheet permeability is roughly proportional to the fourth power of the fibre thickness. This result emphasizes the continued need for the measurement of fibre cross-sectional morphology in paper after papermaking operations in order to predict properties such as air permeability.

ACKNOWLEDGEMENTS

The authors wish to thank Drs. Reza Amiri and Ho Fan Jang for the use of unpublished data and Sylvie St-Amour for the image analysis measurements.

REFERENCES

1. D. Qi and T. Uesaka. Numerical experiments on paper-fluid interaction – permeability of a 3-D anisotropic fibre network. *J. Mater. Sci.* **31**: 4865–4870, 1996.
2. U. Aaltosalmi, M. Katalja, A. Koponen, J. Timonen, A. Goel, G. Lee and S. Ramaswamy. Numerical analysis of fluid flow through fibrous porous materials. *JPPS*, **30**(9): 251, 2004.
3. J. Happel. Viscous flow relative to arrays of cylinders. *AIChE J.* **5**, 174–177, 1959.
4. G.R. Brown. Creeping flow of fluids through assemblages of elliptic cylinders and its applications to the permeability of fiber mats, Ph.D. Thesis, The Institute of Paper Chemistry, Appleton, Wisconsin, 1975.
5. L. Nilsson and S. Stenstrom. A study of the permeability of pulp and paper. *Int. J. Multiphase Flow* **23**(1): 131, 1997.
6. H.F. Jang and R.S. Seth. Using confocal microscopy to characterize the collapse behaviour of fibres. *Tappi J.* **81**(5): 167, 1998.
7. L. Nilsson. A fiber network model for analyzing three transport processes in sheets of paper. Preprints, *Nordic Drying Conference*, Trondheim, Norway, 2001.
8. D.H. Page and R.S. Seth. The elastic modulus of paper Part II – The importance of fibre modulus, bonding and fibre length. *Tappi* **63**(6): 113, 1980.
9. Yamauchi, T. and Murakami, K. Porosity and gas permeability. Chapter 6 in **Handbook of Physical Testing of Paper, Vol. 2, Second edition**, (eds. J. Borch, M. B. Lyne, R. E. Mark, and C. H. Habeger, Jr., Marcel Dekker, New York, Basel, 2001.

10. F.M. White. Ch. 3 in **Viscous Fluid Flow**, Second Edition, McGraw-Hill, page 120, 1991.
11. H.F. Jang. Unpublished data, Paprican.
12. R.W. Perkins Jr. Mechanical behaviour of paper in relation to its structure. In *50th Anniversary Conference, Paper science and technology the cutting edge*, pp89–111, Appleton, Wisconsin, 1979.
13. J. Görres, R. Amiri, M. Grondin and J.R. Wood. Fibre collapse and sheet structure. In **Products of Papermaking**, *Trans. 10th Fund. Res. Symp.*, (ed. C.F. Baker), pp285–311, London, 1993.
14. W.W. Sampson and S.J. Urquhart. The contribution of out-of-plane pore dimensions to the pore size distribution of paper and stochastic fibrous materials. *J. Porous Mater.* 15:411, 2008.
15. Y. Termonia. Permeability of sheets of nonwoven fibrous media. *Chem. Eng. Sci.* **53**(6):1203, 1998.
16. H.K. Corte and E.H. Lloyd. Fluid flow through paper and sheet structure. In **Consolidation of the Paper Web**, *Trans. 3rd Fund. Res. Symp.*, (ed. F. Bolam), pp981–1011, BPBMA, London, 1966.
17. R.S. Seth. Fibre quality factors in pulps II: The importance of fibre coarseness. In *proc. Materials Research Society Symposium, Materials Interactions Relevant to the Pulp, Paper, and Wood Industries*, Vol. 197, pp.143–161, Materials Research Society, Pittsburgh, Pennsylvania, 1990.
18. H.F. Jang, R.C. Howard and R.S. Seth. Fibre characterization using confocal microscopy – The effect of recycling. *Tappi J.* **78**(12): 131, 1995.
19. N. Gurnagul, P. Shallhorn, I. Omholt and K. Miles. Pressurised high-consistency refining of kraft pulps for improved sack paper products. *Appita J.* **62**(1): 25, 2009.
20. J. Görres, R. Amiri, J.R. Wood and A. Karnis. The apparent density of sheets made from pulp blends. *Tappi J.* **79**(1): 179, 1996.

Transcription of Discussion

A SIMPLE MODEL OF THE AIR PERMEABILITY OF PAPER

Paul Shallhorn and Norayr Gurnagul

FPIInnovations – Paprican Division, 570 St. John's Blvd.,
Pointe-Claire, QC, Canada H9R 3J9

Roger Gaudreault Cascades R&D

Norayr, it might be a trivial question, but the unit usually for Gurley is the number of seconds per hundred millilitres, but you used the opposite, i.e. millilitres per second. Is there a reason?

Norayr Gurnagul

Well, the normal units for Gurley are in air resistance and what we showed is, of course, the air permeability.

Ramin Farnood University of Toronto

Thank you, Norayr, for an interesting paper. My question is regarding your assumptions for the model. I realize that you listed a number of limitations in your model, but I wonder if ignoring pore size distribution is another limitation that perhaps needs to be carefully visited. I know Bill Sampson has a couple of related articles and maybe he would like to make some comment too. You can see from your results that pore size in the in-plane is in essence controlling the permeability, no wonder because they are smaller. If you extend this conclusion to the situation that, when you have a pore size distribution, you will have pores which will be smaller than your ordered structure and those pores will be the ones which control the permeability. I just wanted to ask what you think about this?

Discussion

Norayr Gurnagul

Well, that is a very valid point, Ramin, and in fact we do refer to the work by Bill Sampson. I think, Bill, that you showed that fibre thickness is quite important in determining the pore size distribution and to some extent the permeability?

Bill Sampson University of Manchester (from the chair)

What we found was that the pore height distribution contributes about 70% to any measurement of the pore size distribution obtained by flow resistance. The pore height distribution is controlled by the fibre thickness, so this is entirely consistent with Norayr's results.

Petri Mäkelä Innventia

I wonder if you could comment on the effect of drying restraint on the air permeability and how your model would be able to capture that?

Norayr Gurnagul

Good question. Well, I guess drying restraint would have an impact on the pore size distribution. I can't say any more than that.

Bill Sampson

Through porosity, probably.

Norayr Gurnagul

Yes.

Bill Sampson

You said that you felt the model needed to be extended to take account of fines, but you have taken account of density explicitly and this is influenced by fines. So I wonder if that really is a shortcoming because some of your pulps will have significant fines fractions and yet the prediction is quite reasonable? I think the effect of fillers is another point.

Norayr Gurnagul

Yes. That is a good point. I guess the role of fines in terms of their impact on bonding is probably covered by density, but I guess if there are certain fines that are just acting as kind of a filler or filling voids . . .

Bill Sampson

So, for mechanical pulps maybe?

Norayr Gurnagul

Yes.